ARMA 19–1697

Numerical Investigation on Installation Process of Displacement Pile

Copyright 2019 ARMA, American Rock Mechanics Association

This paper was prepared for presentation at the 53rd US Rock Mechanics/Geomechanics Symposium held in New York, NY, USA, 23–26 June 2019. This paper was selected for presentation at the symposium by an ARMA Technical Program Committee based on a technical and critical review of the paper by a minimum of two technical reviewers. The material, as presented, does not necessarily reflect any position of ARMA, its officers, or members. Electronic reproduction, distribution, or storage of any part of this paper for commercial purposes without the written consent of ARMA is prohibited. Permission to reproduce in print is restricted to an abstract of not more than 200 words; illustrations may not be copied. The abstract must contain conspicuous acknowledgement of where and by whom the paper was presented.

ABSTRACT: The fundamental mechanisms governing the behaviour of displacement piles in sand are not well comprehended, leading to unreliability in design methods. Understanding the soil responses during monotonic jacking can help improve the pile foundation design. This paper presents numerical results of pile installation simulated using the two-dimensional discrete element method (DEM), and the influence of soil properties is investigated. The soil responses was examined in terms of displacement, stress and porosity distributions during monotonic jacking, and the Grid Method (GM) was used during sample preparation. The simulation results show great resemblance to the experimental phenomenon. An interface zone adjacent to the pile shaft is observed to comprise of both varying stress states and volumetric states while the pile-soil interface is being sheared. The horizontal stress that acted on the pile shaft reduced in response to installation.

1. INTRODUCTION

The pile installation process will severely distort the soils surrounding a pile when a pile is pushed into the soils (Liu, Yang, & Wang, 2014; Phuong, Tol, Elkadi, & Rohe, 2016). The conventional methods to investigate the effect of pile installation on the surrounding soils include the laboratory and field testing (e.g. Fonseca (2011); Adejumo and Boiko (2013)), or numerical modelling (finite element method (FEM) and discrete element method (DEM)). The results from the experiments are good to analyse the overall behaviour of soils under the pile installation effect, but conducting experiments will take a lot of cost and time. Compared with the experimental techniques, numerical modelling is becoming an acceptable approach to study the pile installation effect on soils (Duan et al 2018), for example, DEM uses the deformable contacts and the time domain solution of the original equations (Itasca 2018). However, many of previous studies (Huang, Ma, & Lee, 1993; Jiang, Harris, & Zhu, 2007; Jiang, Yu, & Harris, 2006) were based on the small size model. Although three-dimensional simulations of monotonic jacking have also been reported recently (Arroyo, Butlanska, Gens, Calvetti, & Jamiolkowski, 2010; Butlanska Joanna, Arroyo Marcos, Gens Antonio, & O'Sullivan Catherine, 2014), the model sizes of these simulations were even smaller. Hence, the boundary effect on the small size model will become very significant. The objective of this study is to reduce the boundary effect, hence providing more accurate understanding of the granular materials behaviour around the pile. Changes of vertical displacement, porosity, and lateral stresses during the installation were analysed.

2. DESCRIPTION OF DEM MODELLING

Table 1 lists the input parameters used in the DEM simulations, the same as that was used in Duan et al (2018). Regarding to the particles, the density of particles is 2650 kg/m^3 which is the typical sand value in realistic condition. The contact normal stiffness has been chosen at 8e7 N/m. A schematic diagram of the DEM model is shown in Figure 1, which includes a solid rigid pile with a diameter of d_{pile} = 45 mm. For the formation of pile in DEM model, each pile-particle, with radius = 1.125 mm and distance of overlap is 0.2 R_{pile} = 0.225 mm, is used to form the outmost shape of the pile. The dense overlap of these pile particles makes the surface of pile relatively smooth, hence, a model steel pile is created. The pile whose density is 500 kg/m^3 is controlled by force in the following installation tests. The sand particles were

simulated as 2D disk ranging from 4.50 mm to 7.05 mm in diameter, with a mean diameter of 5.85mm. To extract the data from the model, the "measurement circle" function inherent in PFC software has been introduced to measure the porosity and stress of soil elements at different locations surrounding the pile. m_r is the radius of measurement circle and the value is 0.05m.

Table 1. Input parameters for DEM simulations

Density of sand particles (kg/m^3)	2650
Density of particles for pile (kg/m^3)	500
Particle diameters (mm)	Figure 2
Average particle size, d_{50} (mm)	5.85
Model pile diameters, d_{pile} (mm)	45
Model pile length, l_{pile} (mm)	200
Model container width (mm)	2400
Model container depth (mm)	1052.3
Friction coefficient of the particles μ (-)	0.5
Friction coefficient of pile & walls μ (-)	0.5
Particles Young's Modulus, E_p (Pa)	4e7
Contact normal stiffness of pile & particles, k_n (N/m)	8e7
Particle stiffness ratio (k_s/ k_n)	0.25
Contact normal stiffness of walls, k_n (N/m)	6e12
Initial average porosity	0.25
Final average porosity (final equilibrium)	0.185
Bulk unit weight γ bulk (kN/m3)	2115

The 2D-DEM analyses in this investigation were performed by using an increased gravity field of 100 g. The purpose of increasing gravity was to increase the simulation speed. Hence, this model could reach a convergent quasi-static solution in a shorter computational time. It was also found that, under the condition of 100g, the simulation data of this 2D-DEM model matched the same stress level of centrifuge test at 100g. The detailed comparisons of the numerical data and a set of centrifuge test data are shown in Duan and Cheng (2017), Duan and Cheng (2018). The size of this model is double the size in Duan and Cheng (2018) to minimise the boundary effect.

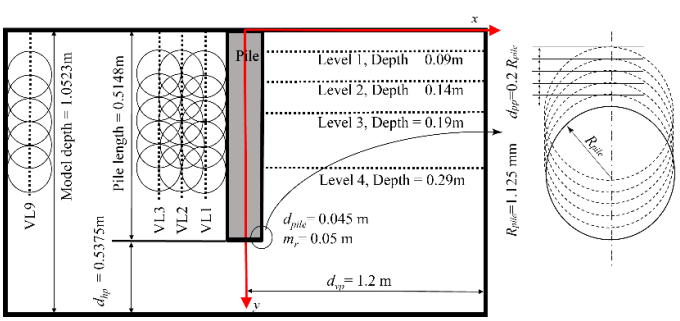

Fig. 1. Schematic drawing of the model (not to scale).

The size and locations of the measurement circles are described in Figure 1. It needs to be highlighted that only half side of results are presented and discussed due to the symmetrical nature of the model. Four levels of depths (the shallowest Level 1 is 0.09 m below pile tip, and the deepest Level 4 is at mid-depth of the pile, i.e. 0.1 m above pile tip) were monitored together with nine observed horizontal locations (VL1, VL2…VL9).

The sand particles were made of discs with a maximum diameter of 7.05 mm, a minimum diameter of 4.5 mm, an average diameter d_{50}=5.85 mm and uniformity coefficient $c_u = d_{60}/d_{10}$= 1.26 (see Figure 2).

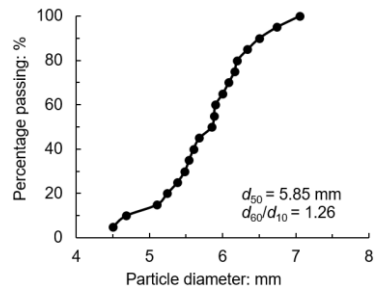

Fig. 2. Average lateral and vertical stress.

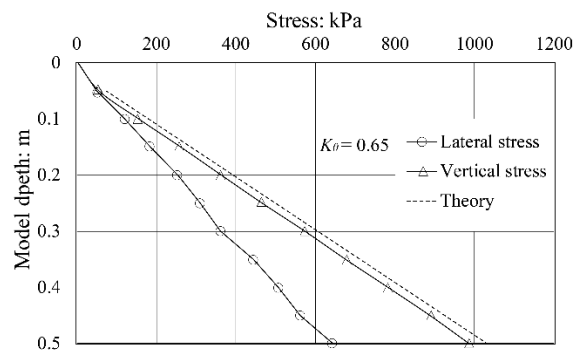

Fig. 3. Average lateral and vertical stress.

Figure 3 shows the distributions of the average lateral and vertical stress distributions and the coefficient of earth pressure (Ko = 0.65). The driven pile was pushed by a stepwise increase of vertical load: 0kN, 20kN, 40kN, 60kN, 80kN, 100kN, 120kN and 140kN. After applying a particular load, the whole 2D-DEM system has been cycled until the sample reaches an equilibrium state. This state could be judged by the ratio of average unbalanced force to average contact force in the system (the value is 1e-5 in this study).

3. RESULTS AND DISCUSSION

Figure 4 shows the contour of vertical particle accumulated displacement. The negative value means the downward accumulated displacement of particles. In regarding to the color, red means the smallest displacement of particles which is about 0.45 mm. In the area where it is far from the pile, the particles can be found to remain almost stationary according to the index of red color. Brown color indicates the particles have been moved downward 4.5 mm. In terms of range of brown color, it expanded quickly from Figure 4 (a) to (d) as the

applied force increased from 0 kN to 60 kN. However, the range of brown color increased slowly from Figure 4 (e) to (f), and the corresponding applied force changed from 80 kN to 140 kN. This trend illustrates that the affected range will not be expanded when the penetration depth has achieved at the certain depth. The brown represents the smallest Y direction displacement. Simultaneously, the light grey means the strongest affected area, and the relevant Y displacement is 45 mm. In contrast to brown color, the light grey color increased slow at the beginning, and developed quickly from Figure 4 (e). The range of yellow near the brown color expresses the 10 mm displacement. At the beginning of pile penetration, the yellow range develop downward mainly. When the applied force is bigger than 80 kN (Figure 4 (e)), the shallow area is going to be affected.

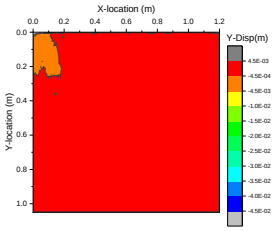

(a) F=0kN (0m)

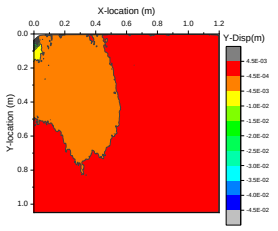

(b) F=20kN (0.04m)

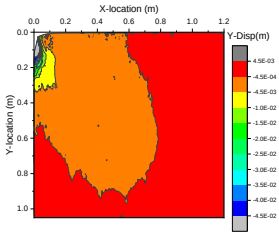

(c) F=40kN (0.09m)

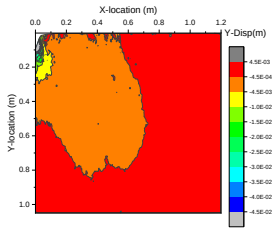

(d) F=60kN (0.11m)

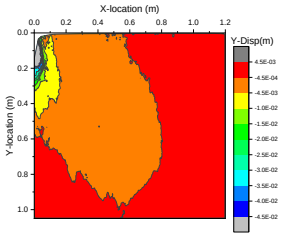

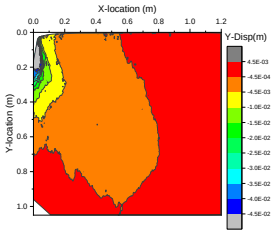

(e) F=80kN (0.13m)

(f) F=100kN (0.16m)

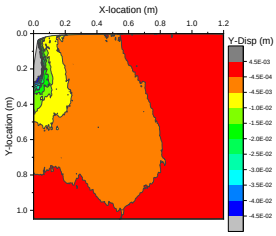

(g) F=120kN (0.18m)

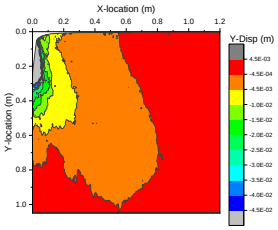

(h) F=140kN (0.22m)

Fig. 4. The Y direction displacement contours under different axial force.

From the development of Figure 4, the lower part of sands will be influenced first due to the pile penetration. After the pile reached at a certain depth, the shallow part of sands begins to be affected. After a period of penetration, the effect of pile tip on the region where the pile tip has passed will fade away. Then, these parts become to experience the shear action which is the principle effect during the pile penetration. This phenomenon indicates that the penetration affects the downwards range and shear action mainly influence the lateral direction.

Figures 5 illustrates the change in porosity and lateral stress at a specific depth of XXX mm below soil surface, and under the particular axial force with respect to 0 kN (i.e. conditions under particular force minus conditions at 0 kN). Porosity and lateral stress have the closed inverse relationship. This connection has been verified in Figure 4, so this DEM model has been proofed to correctly capture the procedure of pile penetration.

It can be seen that the value of lateral stress is more sensitive than porosity. The maximum increase in lateral stress takes place due to the squeezing action of pile tip. Along the pile shaft, the lateral stress decrease obviously is observed as pile tip has passed.

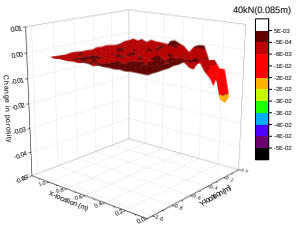

(a) F=40kN

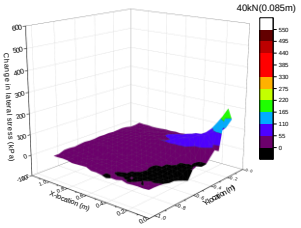

(b) F=40kN

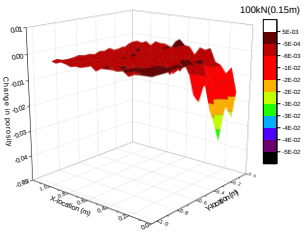

(c) F=100kN

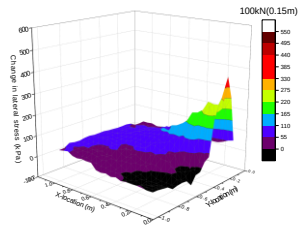

(d) F=100kN

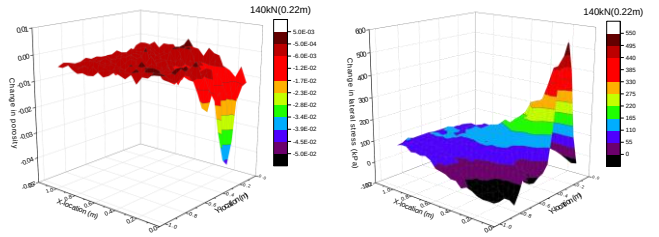

(e) F=140kN (f) F=140kN

Fig. 5. Change in porosity (a, c, e) and lateral stress (b, d, f) of 40 kN, 100 kN and 140 kN with reference at 0 kN

At the certain depth, the radial stress along the pile shaft will affect the pile shaft resistance. This explains the degradation of shaft friction at a given soil horizon with increased pile penetration (friction fatigue).

4. CONCLUSIONS

The process of driven pile installation is investigated numerically based on a 2D DEM model. In addition, the behaviour of influenced zone was analysed. When considering the effect of pile installation, the change in the lateral stress can be observed surrounding the pile. The trend of lateral stress is opposite to the change of porosity. The lateral stress increase at the peak value before the pile tip pass the corresponding depth, and decrease when the pile tip just passes. This analysis captured successfully the formation and evolution of particle flow movement along the pile shaft and below the pile base during the pile installation. This situation can lead to the pile shaft resistance decrease (friction fatigue). The analyses also reveal that the global load-settlement response of the pile to axial loading is closely related and governed by the local behavior in the sand near the pile.

REFERENCES

1. Liu, M., Yang, M., and Wang, H. 2014. Bearing behavior of wide-shallow bucket foundation for offshore wind turbines in drained silty sand. *Ocean Engineering*. 82(82): 169-179.
2. Fonseca, A. V. D. 2011. Effects of the construction method on pile performance: evaluation by instrumentation - part 1: experimental site at the University of Campinas. *Soils & Rocks*. 34(1): 51-64.
3. Adejumo, T. W., and Boiko, I. L. 2013. Effect of Installation Techniques on the Allowable Bearing Capacity of Modeled Circular Piles in Layered Soil. *International Journal of Advanced Technology & Engineering Research*. 2(8): 1536-1542.
4. Cheng, Y. P. 2003. Discrete element simulation of crushable soil. *Géotechnique*. 53(7), 633-642.
5. Huang, A. B., Ma, M. Y., and Lee, J. S. 1993. A micromechanical study of penetration tests in granular material. *Mechanics of Materials*. 16(1–2): 133-139.
6. Jiang, M. J., Harris, D., and Zhu, H. H. 2007. Future continuum models for granular materials in penetration analyses. *Granular Matter*. 9(1-2): 97-108.
7. Jiang, M. J., Yu, H. S., and Harris, D. 2006. Discrete element modelling of deep penetration in granular soils. *International Journal for Numerical & Analytical Methods in Geomechanics*. 30(4), 335-361.
8. Arroyo, M., Butlanska, J., Gens, A., Calvetti, F., and Jamiolkowski, M. 2010. Cone penetration tests in a virtual calibration chamber. Universitat Politècnica De Catalunya, 53(5): 531-536.
9. ButlanskaJoanna, ArroyoMarcos, GensAntonio, and O'SullivanCatherine. 2014. Multi-scale analysis of cone penetration test (CPT) in a virtual calibration chamber. *Canadian Geotechnical Journal*. 51(1): 51-66.
10. Duan, N., Cheng, Y. P., and Xu, X. 2017. Distinct-element analysis of an offshore wind turbine monopile under cyclic lateral load. *Geotechnical Engineering*. 170(6).
11. Duan, N., Cheng, Y. P., and Liu, J. W. 2018. DEM analysis of pile installation effect: comparing a bored and a driven pile. *Granular Matter*. 20(3): 36.